

Modeling and control of Grid connected photovoltaic system using sliding mode control

Abdelkader Belhachemi¹
hachemiaek@gmail

Belarbi Ahmed Wahid¹
baw_dz@yahoo.com

¹ Applied Power Electronics Laboratory Oran University of Science and Technology - Mohamed Boudiaf –

Abstract— Solar PV systems are gaining attraction for energy generation in these days due to its reducing cost and efficiency. The proposed system consists of two main controllers: the DC/DC boost converter to track the maximum power from the PV panels using an application of sliding mode control because it is fast and unconditionally stable and the grid-tied three-phase inverter to control the power active and reactive for achieved the unit power factor in connection point and synchronize a sinusoidal current output with a voltage grid with regulated DC bus voltage. Simulation results are provided to demonstrate the effectiveness of the proposed design and robustness under different operating conditions such as changes in atmospheric conditions.

Keywords-component; Photovoltaic, Maximum power point tracking, MPPT, Sliding mode control, SMC, DC/DC converter , Grid-connected photovoltaic system

I. INTRODUCTION

Due to the extreme dependence on non-renewable traditional fossil fuel energy sources, renewable energy is increasingly in demand recently. Among all renewable energy such as wind energy, fuel cells, ocean energy, etc., solar energy seems to be a promising source of energy.

Photovoltaic cells have a single operating point where the values of the current and voltage of the cell result in a maximum power output[1]. These values correspond to a particular resistance which is equal to the division of the maximum voltage and maximum current. A maximum power point tracker (MPPT) is a device capable of search for the point of maximum power and, using DC-DC converters, extracts the maximum power available by the cell. By controlling the duty cycle of the switching frequency of the converter we can change the equivalent voltage of the cell [2-8]. Multiple types of methods have been designed and implemented to search for this operation point ,which differ in complexity, number of sensors needed for operation, convergence speed, cost-effective range, etc. [9]. Two of the most commonly used MPPT techniques are Perturb and Observe (P & O) and Incremental Conductance (IC). The reason for this popularity is its implementation simplicity and its relatively good performance [10, 11]. Other MPPT algorithms are based on using fractional values of the open circuit voltage and operate the PV module at a fixed percent of this voltage. The main advantages of those

solutions are the low cost and implementation simplicity since they only require a single (voltage or current) sensor [12, 13]; But their efficiency is low compared with the P & O and IC algorithms. In contrasts, techniques based on computational intelligence, such as neural networks and fuzzy logic, offer speed and efficiency in tracking the MPP [14, 15]; however its complexity and implementation costs are high compared with the P & O and IC algorithms. The key technology to overcome both the power quality and grid stability challenges in interfacing the PV system to the grid is the advanced control of the Voltage Source Converter (VSC). In grid-connected PV system, the inverter operates in current control mode where the grid regulates the voltage and frequency at the connection point by setting current reference for the inverter to allow exchange of active and reactive powers. Our objective is to control the active and reactive power to some reference values [16, 17].The power references and the voltage references are then used to set the references for the current controllers. The inverter is supplied from a DC link capacitor. The optimum operating point is highly dependent on the connected load and parameters such as the temperature and irradiance. The Pulse Width Modulation (PWM) inverter expressed in the dq rotating frame there is an inherent coupling between the active and reactive components of the current which makes it difficult to regulate the power injected into the grid from the PV generation system. An effective decoupling strategy based on proportional-integral (PI) controllers is designed to eliminate the interaction between the two current components.

In this paper, a sliding mode control is applied to track maximum power of photovoltaic system. The advantages of this control are various and important: high precision, good stability, simplicity, invariance, robustness etc.... This allows it to be particularly suitable for systems with imprecise model. Often it is better to specify the system dynamics during the convergence mode. This paper is organized as follows: Section IV reviews the modeling of the PV system, in section V, Converters Topology is given, Section VII discusses the control strategy proposed to track the MPP, section IX provides a simulation that shows that the control approach can yield satisfactory results in terms of robustness toward variations in the PV system operating conditions.

II. PROPOSED SYSTEM

The system we propose consists of a PV cells and boost converter that is used for controlling the MPP. The VSI is

used for transforming the DC current into AC current of system frequency, as well as for the active and reactive power control in the system. A schematic overview of the power system with PV cell source is given in Fig.1

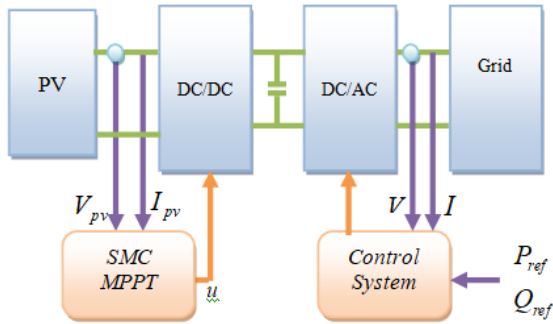


Figure 1 : Proposed system.

III. PV DEVICE MODELING

PV Device will generate electrical power by converting solar irradiation into direct current. The PV system composed of N in series cells and P in parallel cells. Such a series and parallel combination of modules is called a PV array. In the past, there have been different types of models to estimate the non linear equations of the photovoltaic module. Models like Anderson's, Blesser and the most common used the one diode model because it provides a good compromise between the accuracy and the simplicity[16]. All these models present a good approach into estimating the solar cell voltage and currents. The double-diode model is having better accuracy [17, 18]because it takes into account some physical phenomena of semiconductor, viz., charge diffusion and recombination in the space charge layer.

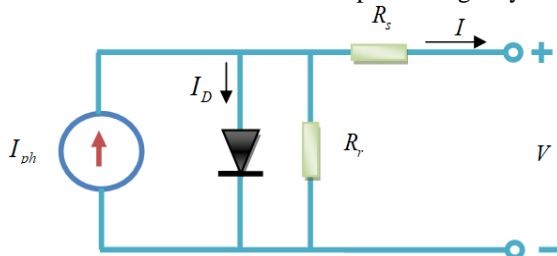


Figure 2. PV module equivalent circuit.

In Fig.2, the current source is used to model the incident solar irradiance, a diode representing the polarization phenomena, a series and parallel resistances to represent the power losses. The mathematical equations describing the cases in Fig.2 are given respectively by:

$$I = I_{ph} - \underbrace{I_{sat} \left(e^{\frac{V}{N_s A V_T}} - 1 \right)}_{I_D} \quad (1)$$

$$I = I_{ph} - I_{sat} \left(e^{\frac{V + IR_s}{N_s A V_T}} - 1 \right) - \frac{V + IR_s}{R_p} \quad (2)$$

$$I = I_{ph} - I_{sat1} \left(e^{\frac{V + IR_s}{N_s V_T}} - 1 \right) - I_{sat2} \left(e^{\frac{V + IR_s}{N_s 2V_T}} - 1 \right) - \frac{V + IR_s}{R_p} \quad (3)$$

Where, I: PV module terminal current (A); I_{ph}: Photo generated current (A); V: PV module terminal voltage (V); R_s: Equivalent series resistance (Ω); R_p: Equivalent parallel resistance (Ω); I_{sat} : Diode saturation current (A); N_s: Number of cells connected in series; V_T: Diode thermal voltage = kT/q; k: Boltzmann's constant (1.3806503 e-23 J/K); T: Temperature (°K); q : Charge of electron (1.60217646 e-19 C); A : Diode ideality factor (1 ≤ A ≤ 2) ;The change of irradiance has an effect on the performance of the PV module according to the following set of equations:

$$I_{sc}(G) = \left(\frac{G}{G_{stc}} \right) I_{sc}(G_{stc}) \quad (4)$$

$$V_{oc}(G) = V_{oc}(G_{stc}) + N_s V_T \log \left(\frac{G}{G_{stc}} \right) \quad (5)$$

IV.CONVERTERS TOPOLOGY:

To pursue the maximum power point (MPPT), DC/DC Converters are most widely applied in photovoltaic systems as an intermediate between the solar cells and the load. Different topologies and different design approaches could be used for DC/DC converters. In this study boost converters is introduced as shown in Figs. 3 , the switching period of "T" and duty cycle "d" for this converter, state equation of voltage results in the Esq. (6) (8).

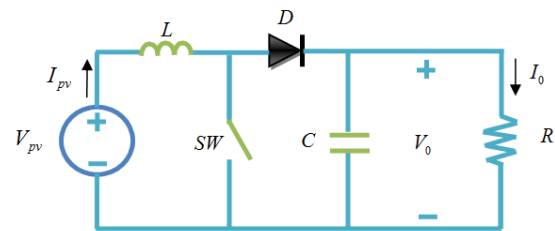


Figure 3. DC/DC boost converter.

$$\frac{dI_L}{dt} = -\frac{1-d}{L} V_0 + \frac{1}{L} V_{pv} \quad (6)$$

Also, the relation between I_L and I_{pv} for each type of converter is as follows:

$$I_L = K I_{pv} \quad (7)$$

In which, K is given as follows:

$$K = 1 \quad (8)$$

V.CONCEPT OF MAXIMUM POWER POINT

Along The maximum power point principle is based on the circuit principle: when the photovoltaic cell's output impedance and the load impedance are equal. The MPP can be affected by climate conditions such as: temperature and irradiance that's why the relationship between voltage and current is non-linear The MPPT principles is to

control the duty cycle for the pulse width modulation block that controls the power converter to deliver maximum power to the load.

VI. SLIDING MODE CONTROLLER

The advantage of this method is its simplicity and robustness in spite of uncertainties in the system and external disturbances and on the other hand it needs relatively less information about the system and also is insensitive to the parametrical changes of the system plus it doesn't need to the mathematical models accurately like classical controllers but needs to know the range of parameter changes for ensuring sustainability and condition satisfactory. The sliding mode control goes through three stages: Choice of surface, Convergence condition and Calculation of the control laws.

The Proposed Sliding Mode Control Approach for MPPT

Fig. 4 shows the I-V characteristic curve of a solar array using sliding mode control method.

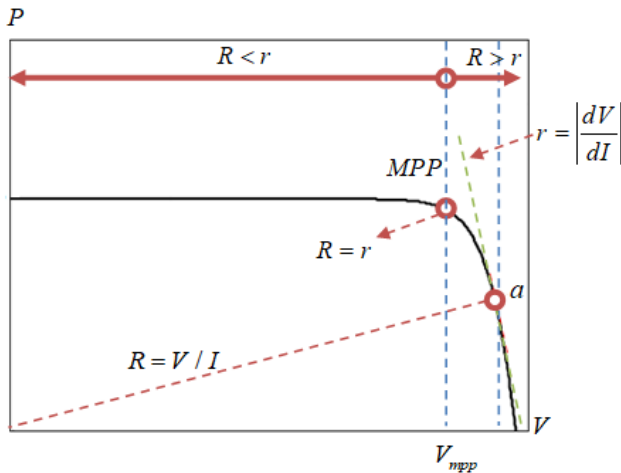


Figure 4. I-V curve of PV array using proposed method.

MPP is calculated by solving Eq. (9):

$$\frac{\partial P_{pv}}{\partial V_{pv}} = \frac{\partial (V_{pv} \cdot I_{pv})}{\partial V_{pv}} = V_{pv} \cdot dI_{pv} + dV_{pv} \cdot I_{pv} = 0 \quad (9)$$

Where:

V_{pv} : The PV voltage, I_{pv} : The PV current

This equation shows that to obtain this point, $(-dV_{pv} / dI_{pv})$ must be equal to (V_{pv} / I_{pv}) . In

This Method, $(-dV_{pv} / dI_{pv})$ is known as instantaneous array resistance "R" and (V_{pv} / I_{pv}) is known as incremental resistance "r". Thus, at maximum power point, the following equation must be satisfied as shown in fig.4:

$$\frac{V_{pv}}{I_{pv}} = \frac{dV_{pv}}{dI_{pv}} \Rightarrow R(I_{pv}) - r(I_{pv}) = 0 \quad (10)$$

Therefore, the sliding surface can be defined based on the error between the instantaneous array resistance (R) and the incremental resistance (r):

$$\sigma = R(I_{pv}) - r(I_{pv}) \quad (11)$$

Now by defining the above surface, control law should be obtained for three different of converters topologies that forces the system to move on the sliding mode surface in a finite time in which the following structure for control input is used as it is used in [24]:

$$U(t) = U_{eq}(t) + U_n(t) \quad (12)$$

Where,

U_{eq} : defines the system's behavior on the sliding surface and known as equivalent control-input

U_n : known as non-linear switching input that moves the state to the sliding surface and keeps the state on the sliding surface in the presence of the uncertainty

U_{eq} , is obtained from the invariance condition and is given as below:

$$(\sigma = 0, d\sigma = 0), \text{ which mean } U = U_{eq} \quad (13)$$

The derivative of the sliding surface Eq. (7) is:

$$d\sigma = \left(\frac{\partial R}{\partial I_{pv}} - \frac{\partial r}{\partial I_{pv}} \right) \cdot \frac{dI_{pv}}{dt} \quad (14)$$

Substituting Eq. (6) into Eq. (23) results in:

$$d\sigma = A \cdot \frac{dI_L}{dt} \quad (15)$$

Where:

$$A = k \left(\frac{\partial R}{\partial I_{pv}} - \frac{\partial r}{\partial I_{pv}} \right) \quad (16)$$

By substituting Esq. (6) into Eq. (11), the time derivative of sliding surface is obtained:

$$d\sigma = A \left[\frac{V_{pv}}{L} - (1-u(t)) \cdot \frac{V_0}{L} \right] \quad (17)$$

Considering Eq. (15) and Eq. (11), the equivalent control-input is obtained as:

$$U_{eq}(t) = 1 - \frac{V_{pv}}{V_0} \quad (18)$$

Now $U_n(t)$ is chosen so that the Lyapunov stability criteria and its chosen as:

$$U_n(t) = \frac{V_{pv}}{V_0} + M \quad (19)$$

Where M is control signal which is calculated through Lyapunov stability criteria (given below). Therefore, the Eq. (16), (17) give the control law defined in Eq. (10) as:

$$U(t) = 1 - M \quad (20)$$

A Lyapunov function and its time derivative are defined as:

$$V = \frac{1}{2}\sigma^2, dV = d\sigma \cdot \sigma \quad (21)$$

If Eq. (11) is substituted into Eq. (18), we get:

$$dV = A \cdot \left[\frac{V_{pv}}{L} - (1-U(t)) \cdot \frac{V_0}{L} \right] \cdot \sigma \quad (22)$$

Substituting Eq. (11) into Eq. (13) gives the following result:

$$dV = \frac{A}{L} \cdot [V_{pv} - MV_0] \cdot \sigma \quad (23)$$

Assume the operating point of the system is 'a' in Fig. 4. Since the gradient is negative, moving the operating point to the right side causes increasing in the current of PV array, which results in decreasing of R and increasing of r, therefore,

$$\frac{\partial R}{\partial I_{pv}} < 0, \frac{\partial r}{\partial I_{pv}} > 0 \quad (24)$$

Also, moving the operating point to the left side causes decreasing in the current of PV array, which results in increasing of R and decreasing of r, therefore,

$$\frac{\partial R}{\partial I_{pv}} > 0, \frac{\partial r}{\partial I_{pv}} < 0 \quad (25)$$

Thus, the sign of "A" in Eq. (9) is always negative, for positive sliding surface we have:

$$\sigma > 0 \Rightarrow \frac{V_{pv}}{I_{pv}} > \left| \frac{dV_{pv}}{dI_{pv}} \right| \quad (26)$$

For a positive parameter a, we have:

$$\sigma > 0 \Rightarrow \left(\frac{V_{pv}}{I_{pv}} \right)^a > \left| \frac{dV_{pv}}{dI_{pv}} \right|^a \quad (27)$$

Multiplying above inequality in $\frac{(V_{pv})^{1-a} (I_{pv})^a}{V_0} > 0$ results in:

$$\begin{aligned} \sigma > 0 \Rightarrow \\ \Rightarrow \left(\frac{(V_{pv})^{1-a} (I_{pv})^a}{V_0} \right) \left(\frac{V_{pv}}{I_{pv}} \right)^a > \left(\frac{(V_{pv})^{1-a} (I_{pv})^a}{V_0} \right) \left| \frac{dV_{pv}}{dI_{pv}} \right|^a \end{aligned} \quad (28)$$

This simplifies as:

$$\sigma > 0 \Rightarrow \left(\frac{V_{pv}}{I_{pv}} \right) > \left(\frac{(V_{pv})^{1-a} (I_{pv})^a}{V_0} \right) \left| \frac{dV_{pv}}{dI_{pv}} \right|^a \quad (29)$$

Similar to $\sigma > 0$, for $\sigma < 0$ we get:

$$\sigma < 0 \Rightarrow \left(\frac{V_{pv}}{I_{pv}} \right) < \left(\frac{(V_{pv})^{1-a} (I_{pv})^a}{V_0} \right) \left| \frac{dV_{pv}}{dI_{pv}} \right|^a \quad (30)$$

Based on Esq. (27) and (28), the control law M can be chosen as:

$$M = \left(\frac{(V_{pv})^{1-a} (I_{pv})^a}{V_0} \right) \left| \frac{dV_{pv}}{dI_{pv}} \right|^a \quad (31)$$

Therefore, for positive and negative sliding surface we have:

$$\sigma > 0 \Rightarrow \left(\frac{V_{pv}}{I_{pv}} \right) > M \Rightarrow [V_{pv} - MV_0] > 0 \quad (32)$$

$$\Rightarrow \sigma \cdot [V_{pv} - MV_0] > 0$$

$$\sigma < 0 \Rightarrow \left(\frac{V_{pv}}{I_{pv}} \right) < M \Rightarrow [V_{pv} - MV_0] < 0 \quad (33)$$

$$\Rightarrow \sigma \cdot [V_{pv} - MV_0] > 0$$

By considering Eq. (28) and since $A < 0$, the time derivative of Lyapunov function in Eq. (21) is negative ($dV = d\sigma \cdot \sigma < 0$). Thus, by substituting Eq. (27) into Eq. (18), the control input is obtained as follows which forces the system to move on the sliding mode surface in a finite time:

$$U(t) = 1 - \left(\frac{(V_{pv})^{1-a} (I_{pv})^a}{V_0} \right) \left| \frac{dV_{pv}}{dI_{pv}} \right|^a \quad (34)$$

Since the range of duty cycle must lie in $0 < d < 1$, the real control signal proposed as:

$$d = \begin{cases} 0 & U(t) \leq 0 \\ U(t) & 0 < U(t) < 1 \\ 1 & 1 \leq U(t) \end{cases} \quad (35)$$

VII. GRID-CONNECTED INVERTER

In this paper we applied two decoupling methods: feed forward and feedback decoupling method for current control. Photovoltaic inverter mainly controls that capacitance voltage is stability in DC side bus and output current accords with grid-connected conditions [19]. The mathematical model in dq coordinates shown below.

$$\begin{cases} L \frac{dI_d}{dt} = -RI_d + \omega LI_q - S_d U_{DC} + U_d \\ L \frac{dI_q}{dt} = -RI_q - \omega LI_d - S_q U_{DC} + U_q \\ C \frac{dI_{DC}}{dt} = \frac{3S_d I_d}{2} + \frac{3S_q I_q}{2} - I \end{cases} \quad (36)$$

Where;

I_{DC} is the current on DC side capacitor of inverter;

U_{DC} is input DC voltage of inverter;

S_d, S_q is the dq component of S_i in the dq coordinate respectively. When $S_i = 0$, it expresses that below tube will break over in the i phase; when $S_i = 1$, it expresses that above tube will break over in the i phase.

U_d, U_q are the dq component of grid voltage, I_d, I_q are the dq component of output current. Due to the approximate constant of the grid voltage, it can make d axis in the synchronous rotating dq coordinate system orientate in grid voltage vector us direction to simplify calculation, so the dq component of grid voltage is: $U_d = U_s, U_q = 0$, and substitute them into formula (36) to get :

$$\begin{cases} U_d^* = -\left(L \frac{dI_d}{dt} + I_d R\right) + \omega L I_q + U_s \\ U_q^* = -\left(L \frac{dI_q}{dt} + I_q R\right) - \omega L I_d \end{cases} \quad (37)$$

Where;

U_d^*, U_q^* are the dq component of AC voltage in inverter. $U_d^* = S_d U_{DC}, U_q^* = S_q U_{DC}$. In order to eliminate dq axial current coupling and eliminate grid voltage disturbance, it introduces current feedback $\omega L I_q, -\omega L I_d$ to decouple [19], and introduces grid voltage to Feed forward compensate, thus it fulfills the dq axis current independent control.

$$\begin{cases} P = U_d I_d + U_q I_q = U_s I_d \\ Q = U_q I_d + U_d I_q = -U_s I_q \end{cases} \quad (38)$$

I_d^* Value determines the active power, also its symbol decides to flow direction of active power. Reactive current component $I_q^* = 0$, it can realize rectifier and inverter at power factor as 1.

VIII. SIMULATION RESULTS

In this section, a set of simulation tests have been performed for 1 sec, using Matlab –Simulink environment. To demonstrate the performance of SMC based MPPT technique the SIMULINK model of a system is developed. At first, the simulation is run under Standard Test Condition with irradiance $G=1000 \text{ W/m}^2$ and operating temperature of 25°C then The results obtained at STC are as shown in Figure 6. Then a changes of solar irradiance is applied

Steady Operation

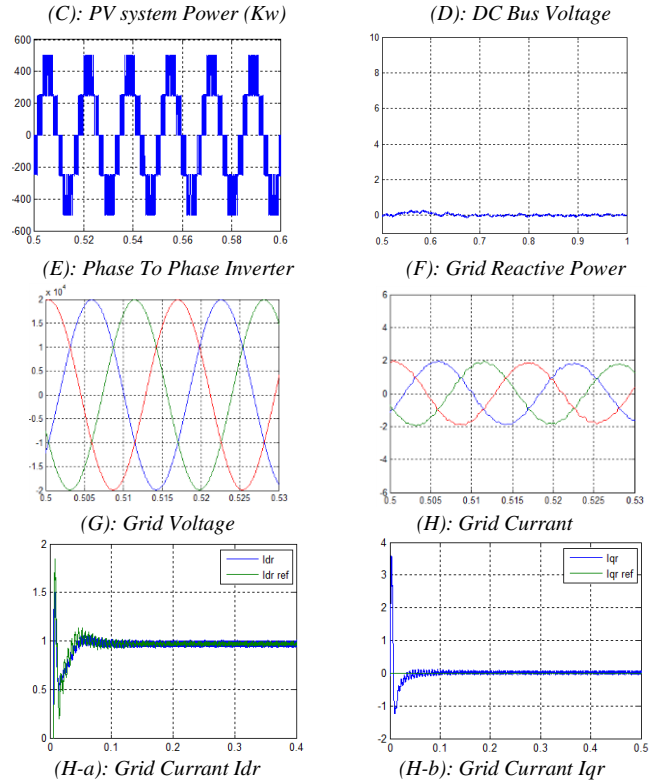
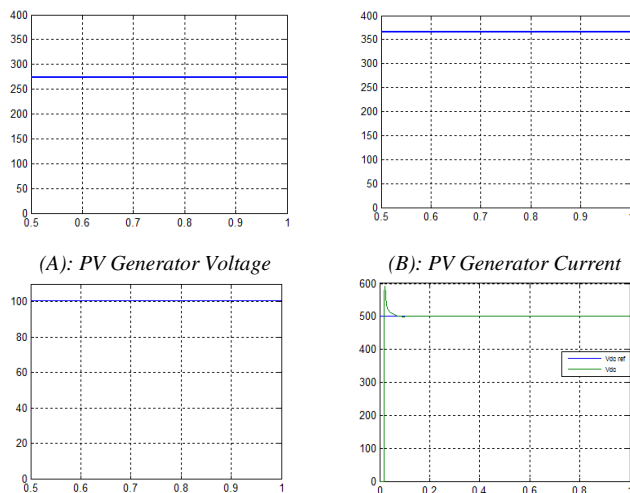


Figure. 5 System voltage, current and power time response under the STC (1000 W/m2).

Reference tracking

In order to evaluate the MPPT control strategy proposed in this paper. We proposed a solar intensity changes at different values of irradiances as shown in Fig (6).

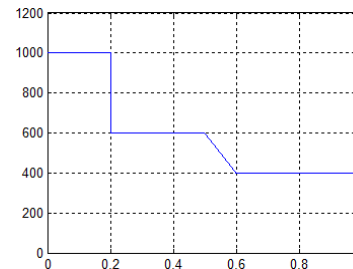
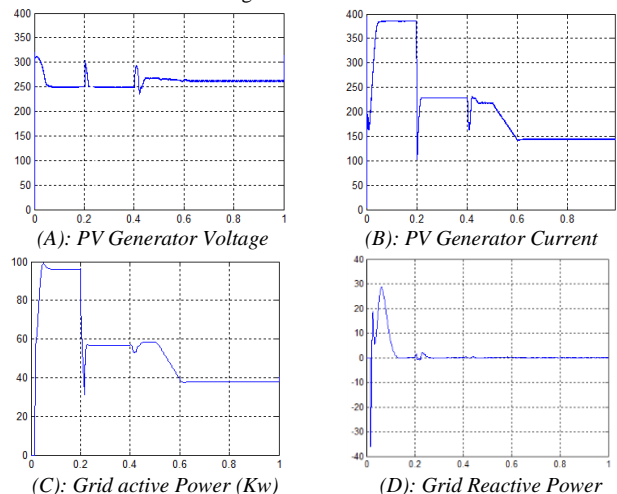


Figure. 6 Irradiance Profile



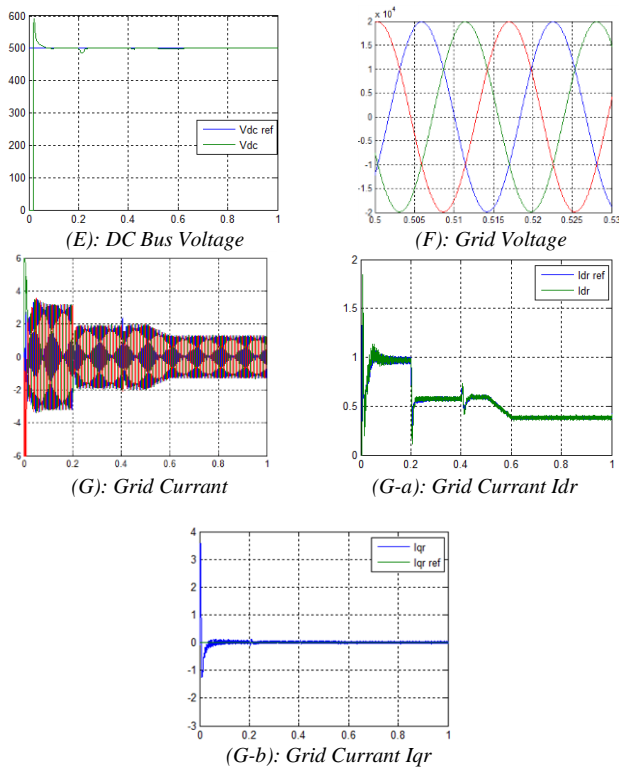


Fig. 7 PV system voltage, current and power time response under the STC profile.

Fig.5 shows that under the STC, the controller achieves the MPP at 1000 W/m^2 corresponding to the peak value of the PV system. And it's also shows the voltage and current at the MPP. The voltage at DC bus is regulated to be 500V. In the second simulation, the irradiance is changing with time, Fig.6 illustrates that the proposed MPP controller maintains the power at its maximum with different irradiance values, and the response time is relatively fast. Instantly, after the irradiance change the control sense the new MPP and re-optimizing again with a different point, with that the controller is able to track of the maximum power. This situation models a transient effect of a cloud blocking the incident irradiance from the PV system. The instantaneous irradiance change imposed on the PV system in this simulation may be much faster than a real world scenario, but it gives an idea of the time it takes for the controller to respond to a change in the irradiance. The proposed MPP tracking successfully scans for the MPP in a relatively short time under varying weather conditions with fast convergence. When solar irradiance is changing, DC bus voltage is either less or higher than 500 V so the dc bus regulator must act to maintain the DC bus voltage constant (at 500 V). In figure 7-E the DC bus voltage controller has insure a constant voltage that make PV system able to feed the inverter and the load, Fig. 7-C-D shows simulation results of active and reactive powers at the AC bus for compare with the reference values by inverter DC-AC. The inverter control is based on a decoupled control of the active and reactive powers. Fig. 7-G shows the current injected into the main utility and the grid side voltage. As it can be noted, the voltage and current are in phase which means that the MP extracted from the PV array can pass into the DC-AC grid-side inverter as the whole system operates at unity

power factor ($Q=0$) with no reactive power exchange. By applying the inverse Park transformation to d,q current vector components, the phase current references are obtained. These are passed to a PI controller, which outputs the pulses to drive the inverter switches. The output line voltage of the inverter is shown in Fig. 7-F.

IX. CONCLUSION

This paper presents an analysis and design of a MPPT control using sliding mode control. This solution is aimed at performing a fast MPPT action on PV systems using the slope of the derivative of the voltage with respect to the current in order to reach the maximum power point. The main concluding remarks are summarized as follows:

- Fast response, good transient performance and sensitivity to variations in external disturbances.
- A simple robust control algorithm that has the advantage to be easily implantable in calculator.
- The disadvantage of this technique is chattering which is generally undesirable because it adds a high frequency components to the spectrum of the GPV voltage and current. To overcome this drawback, high order sliding mode control or a combination with techniques like fuzzy sliding mode should be considered... etc. The vector control strategy of power decoupling makes PV inverter output a high quality power to meet grid-connected requirements, which provides the reliable simulation platform and important technical parameters for designing grid-connected photovoltaic inverter.

References

- [1] A. Durgadevi, S. Arulselvi, S.P. Natarajan, Photovoltaic modeling and its characteristics, 2011 International Conference on Emerging Trends in Electrical and Computer Technology, 2011, pp. 469-475.
- [2] H.L. Jou, W.J. Chiang, J.C. Wu, A Novel Maximum Power Point Tracking Method for the Photovoltaic System, 2007 7th International Conference on Power Electronics and Drive Systems, 2007, pp. 619-623.
- [3] S. Lalouni, D. Rekioua, T. Rekioua, E. Matagne, Fuzzy logic control of stand-alone photovoltaic system with battery storage, Journal of Power Sources 193(2) (2009) 899-907.
- [4] S. Ould-Amrouche, D. Rekioua, A. Hamidat, Modelling photovoltaic water pumping systems and evaluation of their CO₂ emissions mitigation potential, Applied Energy 87(11) (2010) 3451-3459.
- [5] Z. Salameh, D. Taylor, Step-up maximum power point tracker for photovoltaic arrays, Solar Energy 44(1) (1990) 57-61.
- [6] V. Salas, E. Olías, A. Barrado, A. Lázaro, Review of the maximum power point tracking algorithms for stand-alone photovoltaic systems, Solar Energy Materials and Solar Cells 90(11) (2006) 1555-1578.
- [7] A. Yazdani, P.P. Dash, A Control Methodology and Characterization of Dynamics for a Photovoltaic (PV) System Interfaced With a Distribution Network, IEEE Transactions on Power Delivery 24(3) (2009) 1538-1551.
- [8] S. Zhou, L. Kang, J. Sun, G. Guo, B. Cheng, B. Cao, Y. Tang, A novel maximum power point tracking algorithms for stand-alone photovoltaic system, International Journal of Control, Automation and Systems 8(6) (2010) 1364-1371.
- [9] J. Qi, Y. Zhang, Y. Chen, Modeling and maximum power point tracking (MPPT) method for PV array under partial shade conditions, Renewable Energy 66 (2014) 337-345.
- [10] G. Petrone, C.A. Ramos-Paja, G. Spagnuolo, M. Vitelli, Granular control of photovoltaic arrays by means of a multi-output Maximum Power Point Tracking algorithm, Progress in Photovoltaics: Research and Applications 21(5) (2013) 918-932.
- [11] T. Esmar, P.L. Chapman, Comparison of Photovoltaic Array Maximum Power Point Tracking Techniques, IEEE Transactions on Energy Conversion 22(2) (2007) 439-449.

- [12] J. Ahmed, Z. Salam, A Maximum Power Point Tracking (MPPT) for PV system using Cuckoo Search with partial shading capability, *Applied Energy* 119 (2014) 118-130.
- [13] J. Ahmad, A fractional open circuit voltage based maximum power point tracker for photovoltaic arrays, 2010 2nd International Conference on Software Technology and Engineering, 2010, pp. V1-247-V1-250.
- [14] N. Khaehintung, A. Kunakorn, P. Sirisuk, A novel fuzzy logic control technique tuned by particle swarm optimization for maximum power point tracking for a photovoltaic system using a current-mode boost converter with bifurcation control, *International Journal of Control, Automation and Systems* 8(2) (2010) 289-300.
- [15] C.S. Chiu, Y.L. Ouyang, Robust Maximum Power Tracking Control of Uncertain Photovoltaic Systems: A Unified T-S Fuzzy Model-Based Approach, *IEEE Transactions on Control Systems Technology* 19(6) (2011) 1516-1526.
- [16] S.B. Kjaer, J.K. Pedersen, F. Blaabjerg, A review of single-phase grid-connected inverters for photovoltaic modules, *IEEE Transactions on Industry Applications* 41(5) (2005) 1292-1306.
- [17] P.S. Bimbhra, *Power Electronics*, Khanna Publishers.
- [18] M. Barnes, J. Kondoh, H. Asano, J. Oyarzabal, G. Ventakaramanan, R. Lasseter, N. Hatzigiorgiou, T. Green, Real-World MicroGrids-An Overview, 2007 IEEE International Conference on System of Systems Engineering, 2007, pp. 1-8.
- [19] B. Wei, Y. Zhongdong, Study on AC-Excited Control Strategy of Doubly-Fed VSCF Wind Power Generation System, 2009 International Conference on Energy and Environment Technology, 2009, pp. 837-840.

Creative Commons Attribution License 4.0 (Attribution 4.0 International, CC BY 4.0)

This article is published under the terms of the Creative Commons Attribution License 4.0

https://creativecommons.org/licenses/by/4.0/deed.en_US